AADE-15-NTCE-06

Nanoparticle Modified Smart Oil Well Cement for Monitoring Cementing Applications

Cumaraswamy Vipulanandan and Ahmed Mohammed, CIGMAT- University of Houston

Abstract

During cementing operation, it is critical to determine the location of cement slurry between the casing and formation, depth of the circulation losses and fluid loss, setting of cement in place and performance of the cement after hardening. Recent case studies on oil well failures have clearly identified some of the cementing issues that resulted in various types of delays in the cementing operations. At present there is no technology available to monitor cementing operations in real time from the time of placement through the borehole service life. Also, there is no reliable method to determine the length of the competent cement supporting the casing.

In this study, smart cement with 0.38 and 0.54 water-to-cement ratio (w/c) was modified with iron nanoparticles (NanoFe) to have better sensing properties, so that its behavior can be monitored at various stages of construction and during the service life of wells. A series of experiments evaluated well smart cement behavior with and without NanoFe in order to identify the most reliable sensing properties that can also be relatively easily monitored. Tests were performed on the smart cement from the time of mixing to hardened state behavior. During the initial setting the electrical resistivity changed with time based on the w/c and the amount of NanoFe used to modify smart oil well cement. The shear thinning behavior of the smart cement slurries with and without NanoFe at different w/c ratio and temperatures have been quantified using the hyperbolic model and compared with three material parameters, Vocadlo model. The results showed that the hyperbolic model predicated the shear thinning relationship between the shear stress and shear strain rate of the NanoFe modified smart cement slurries very well. Also the hyperbolic model has a maximum shear stress limit were as the other model did not have a limit on the maximum shear stress. Based on the hyperbolic model the maximum shear stresses with w/c ratio of 0.34 and 0.54 modified with 1% NanoFe at temperature of 25^{o}C were 236 Pa and 74 Pa respectively. A new quantification concept has been developed to characterize cement curing based on electrical resistivity changes in the first 24 hours and 7 days of curing. When cement was modified with 0.1% of conductive filer (CF), the piezoresistive behavior of the hardened smart cement was improved without affecting the rheological and setting properties of the cement based on the w/c ratio and the NanoFe content. The test results showed that NanoFe reduced the electrical resistivity of the smart cement slurries. The 1% of NanoFe also affected the rheological properties and the piezoresistive behavior of the smart cement. . The RI_{24hr} for the smart cement with NanoFe decreased with the amount of NanoFe. Addition of 1% NanoFe increased the compressive strength of the smart cement with w/c ratio of 0.38 and 0.54 by 3% and 15% after 1 day of curing respectively. For the smart cement (w/c=0.38) modified with NanoFe, the resistivity change at peak stress was over 2500 times higher than the change in the compressive strain. A linear correlation was obtained between the RI_{24hr} and the compressive strength of the modified smart cement based on the w/c and curing time.

Introduction

As Deepwater exploration and production of oil and gas expands around the world, there are unique challenges in well construction beginning at the seafloor. Recent case studies on cementing failures have clearly identified several issues that resulted in various types of delays in the cementing operations. Also preventing the loss of fluids to the formations and proper well cementing have become critical issues in well construction to ensure wellbore integrity because of varying down hole conditions (Eoff et al. 2009; Labibzadeh et al. 2010). Moreover, the environmental friendliness of the cements is a critical issue that is becoming increasingly important (Thaemlitz et al. 1999; Dom et al. 2007). Lack of cement returns may compromise the casing support, and excess cement returns can cause problems with flow and control lines (Fuller et al. 2002; Gill et al. 2005). Hence there is a need for monitoring the cementing operation in real time. Free ions in the cement slurry have significant effect on electrical resistivity of samples. According to the literature conductivity of cement is mostly related to the three main parameters which are ion concentration, the number of charges per ion and the equivalent ionic conductivity it should be noted according to current experimental results other parameters that has significant effect on resistivity of cement during hydration are curing temperature, curing condition, weight loss during curing and method of resistivity measurement, two probe of four probe testing and frequency of measurement.

Two studies done during the period of 1971 to 1991 and 1992 to 2006 clearly identified cement failures as the major cause for blowouts (McCarter 1996). Cementing failures increased significantly during the second period of study when 18 of the 39 blowouts were due to cementing problem (McCarter 1996).

Electrical resistivity measurement has been applied by many researches on concrete and other cementing applications (McCarter 2006), but there are no reports in the literature of electrical resistivity measurements for characterizing oil well cement. Electrical response characteristics measurement has appropriate sensitivity in monitoring the characteristics of cementitious materials (Mc Carter et al. 1991). The advantages in using this technique include its accuracy, ease of testing and procedures, and nondestructive characteristics (Li et al. 2003). Additionally, this method can be used for monitoring the long term behavior of cement in practice. Electrical resistivity of cement is affected by a number of factors, such as pore structure (continuity and tortuosity), pore solution composition, cementitious content, water-to-cement ratio (w/c), moisture content, and temperature (Polder et al. 2001). Moreover, electrical resistivity of cement is dramatically affected by admixtures, due to the resistivity contrast between cement and the admixture substances. Vipulanandan et al. (2006-2014) have studied the change in electrical resistivity with applied stress, referred to as piezoresistive behavior of modified cementitious and polymer composites.

Objectives

The overall objective of the study was to determine the effect of NanoFe on the behavior of smart oil well cement. The specific objectives are as follows:

(i) Investigate the effect of w/c and NanoFe on the rheological and electrical properties of smart oil well cement.

(ii) Quantify the effect of NanoFe on the piezoresistive behavior of smart cement.

Materials and Methods

Smart Cement

Commercially available oil well cement (Class H cement) was modified with additives to make it a piezoresistive material.

Iron Nanoparticles (NanoFe)

Commercially available nano iron was used in this study. Based on the manufacture's data sheet the particle size was 30 nm, bulk density of 0.25 gm/cc and surface area of 38 m^2/gm.

Cement Samples

The samples were prepared according to the API standards. Smart cement with a w/c ratio of 0.38 and 0.54 were used in this study. Four series of cement slurries without and with 1% of NanoFe were prepared.

After mixing, specimens were prepared using cylindrical molds with a diameter of 2 inches and a height of 4 inches. Two conductive wires were placed in all of the molds which were 5 cm apart. All specimens were capped to minimize moisture loss and were cured up to the 28 days for the piezoresistivity test under compressive loading.

Rheological Tests

Rheological properties determine the ability of cement to be pumped. The rheology tests were performed by utilizing a rotational viscometer at room pressure and temperature at rpms ranging from 3 to 600 rpm, and related shear stresses were recorded. The viscometers were calibrated using several standard solutions.

Electrical Resistivity

Two different instruments were used to measure the electrical resistivity of the smart cement.

(i) Conductivity Probe

Commercially available conductivity probe was used to measure the conductivity (inverse of electrical resistivity) of the fluids. In the case of cement, this meter was used during the initial curing of the cement. The conductivity measuring range was from 0.1μS/cm to 1000 mS/cm representing a resistivity of 10,000 Ω.m to 0.1 Ω.m.

(ii) Digital Resistivity Meter

Digital resistivity meter measured the resistivity of fluids, slurries and semi-solids with resistivity in the range of 0.01 Ω-m to 400 Ω-m. Both of the electrical resistivity devices were calibrated using standard solution. Based on past studies, electrical resistivity was selected the monitoring parameter to quantify the performance of modified cement during curing and hardening process (Vipulanandan et al. 2014 (a) and (b)). Further, Electrical resistance was measured using LCR meter during the curing time. To minimize the contact resistances, the resistance was measured at 300 kHz using two-wire method. Each specimen was calibrated to obtain the electrical resistivity (ρ) from the measured electrical resistance (R) based on the Eqn.1.

$$R = \rho * \left(\frac{L}{A}\right) = \rho K \quad (1)$$

where L is the distance between the wires, A is the cross-sectional area through which the current is flowing, and L/A is called the geometry factor. In addition to geometry, other interfacial factors are important in obtaining electrical resistivity from electrical resistance. Due to the voltage present during electrical resistance measurement, electric polarization occurs as the resistance measurement is made continuously. The polarization results in an increase in the measured resistance (Chung et al 2001). Hence, L/A in Eqn.1 is replaced by an experimentally found calibration factor (K). Normalized change in resistivity with the changing conditions can be represented as follows:

$$\frac{\Delta\rho}{\rho} = \frac{\Delta R}{R} \quad (2)$$

In general total represent resistivity (ρ) is used to the composition and curing characteristics. The incremental resistivity (Δρ) is used as a monitoring tool.

Compression Test

Compressive strength of cement determines the ability of cement to stabilize the casing in the wellbore. The cylindrical specimen was capped and tested at a predetermined controlled displacement rate. Compression tests were performed on cement samples after 1 and 28 days of curing using a hydraulic compression machine.

Piezoresistivity Test

Piezoresistivity describes the change in electrical resistivity of a material under pressure. Since oil well cement serves as a pressure-bearing part of wells in real applications, the piezoresistivity of smart cement with and without NanoFe was investigated under compressive loading. During each compression test, electrical resistance was measured in the stress axis. To eliminate the polarization effect, alternating current (AC) resistance measurements were made using a LCR meter at a frequency of 300 kHz. Furthermore, changes in resistivity were related to the applied stress.

Results and Discussions

Modelling

(i) Vocadlo model

Due to the shear-thinning behavior of the cement slurries Bingham plastic model was not an accurate model to estimate the shear stress - shear strain rate relationship. The advantage of the proposed model is its higher accuracy especially at higher strain shear strain rates. A comparison of the proposed model with the Vocadlo model (Eqn. 3) which is being used in industry is summarized in Fig. 3.

$$\tau = [\tau_{o1}^{\frac{1}{n}} + k^{\frac{1}{n}} * \dot{\gamma}^{0.5}]^{1/n} \quad (3)$$

when $\dot{\gamma} \to \infty \Rightarrow \tau_{\max.} = \infty$

(ii) Hyperbolic model

To predict the shear strain rate - shear stress relationship a hyperbolic model was proposed and fitted with the experimental data (Vipulanandan and Mohammed 2014). The developed hyperbolic model is presented in Eqn. 4 as follows:

$$\tau = \tau_{02} + \frac{\dot{\gamma}}{A + \dot{\gamma}B} \quad (4)$$

where τ_{02} is the yield stress at zero shear strain rate (Pa), $\dot{\gamma}$ is the shear strain rate (s^{-1}) and A and B are the hyperbolic model parameters. Experimental data and hyperbolic prediction for smart cement slurries are shown in Fig. 2.

when

$$\dot{\gamma} \to \infty \Rightarrow \tau_{\max} = \frac{1}{B} + \tau_o \quad (5)$$

Rheological properties

Smart cement slurries with w/c ratio of 0.38 and 0.54 at two different temperatures showed significantly different rheological properties. However, regardless of the NanoFe percentage and temperature, all slurries exhibited non-Newtonian and shear-thinning behavior as shown in Fig. 1.

Rheological Models

Shear stress – shear strain rate relationships were predicated using the hyperbolic model and compared with Vocadlo model as shown in Fig. 1 and Fig. 2.

(i) Vocadlo Model

(a) NanoFe=0%

The shear thinning behavior of smart cement slurry with w/c ratio of 0.38 and 0.54 and NanoFe of 0% at two different temperatures 25°C and 85°C were modeled using the Vocadlo model (Eqn. (3)) up to a shear strain rate of 1024 s^{-1} (600 rpm). The coefficient of determination (R^2) was greater than 0.97 as summarized in Table 1. The root mean square of error (RMSE) varied between 5.6 Pa and 11.1 Pa based on the temperature, NanoFe content and w/c ratio as summarized in Table 1. The yield stress (τ_{o1}) for the cement slurry with w/c ratio of 0.38 and 0.54 at temperature of 25°C were 21.3 Pa and 18.5 Pa respectively, with increasing the temperature of the slurry to 85°C, the yield stress increased to 42.5 Pa and 37.5 Pa respectively, a 97% and 150% increase respectively. The model parameter k for the cement slurry with w/c ratio of 0.38 and 0.54 at temperatures of 25°C and 85°C varied between 3.88 $Pa.s^n$ and 21.3 $Pa.s^n$ based on the temperature, NanoFe content and w/c ratio as summarized in Table 1. The model parameter n for the cement slurry varied between 0.31 and 0.75 based on the temperature, NanoFe content and w/c ratio as summarized in Table 1.

(b) NanoFe=1%

Using the Vocadlo model (Eqn. (3)), the relationships between shear stress with shear strain rate of for smart cement slurry mud with NanoFe of 1% at 25°C and 85°C of temperature and with w/c ratio of 0.38 and 0.54 were modeled. The coefficient of determination (R^2) was varied between 0.97 and 0.99 as summarized in Table 1. The root mean square of error (RMSE) varied from 2.59 Pa to 11.1 Pa as summarized in Table 1. The yield stress (τ_{o1}) of the cement slurry with w/c ratio of 0.38 and 0.54 at 25°C were 34.1 Pa 21.3 Pa and increased to 47.1 Pa and 41.1 Pa with increasing the temperature to 85°C, a 38% and 92% increase as summarized in Table 1. The model parameter k for the cement slurry with w/c ratio of 0.38 and 0.54 at 25°C and 85°C varied between 2.9 $Pa.s^n$ and 56.7 $Pa.s^n$ based on the temperature, NanoFe content and w/c ratio. The model parameter n for cement slurry decreased with increasing the temperature to 85°C as summarized in Table 1.

(ii) Hyperbolic Model

(a) NanoFe=0%

The shear thinning behavior of the smart cement slurry with NanoFe of 0% at 25°C and 85°C were modeled using the Hyperbolic model (Eqn. (4)). The coefficient of determination (R^2) was greater than 0.97 as summarized in Table 1. The root mean square of error (RMSE) varied between 0.03 Pa and 9.9 Pa respectively as summarized in Table 1. The yield stress (τ_{o2}) of the smart cement slurry with w/c ratio of 0.38 and 0.54 at 25oC was 22.3 Pa and increased to 53.2 Pa and 36.1 Pa with increasing the temperature to 85°C, a 175% and 137% increase as summarized in Table 1. The model parameter A for the smart cement slurry with w/c ratio of 0.38 and 0.54 at 25°C and 85°C varied between 0.32 Pa.s^{-1} and 4.7 Pa.s^{-1} based on the temperature, NanoFe content and w/c ratio as summarized in Table 1. The model parameter B for the smart cement slurry with w/c ratio of 0.38 and 0.54 at 25°C and 85°C was 0.003 Pa^{-1} 0.01 Pa^{-1} and 0.02 Pa^{-1} and 0.003 Pa^{-1} respectively, a 133% reduction with increasing the temperature to 85°C as summarized in Table 1.

(b) NanoFe=1%

Using the Hyperbolic model (Eqn. (4)), the relationships between shear stress with shear strain rate of the smart cement slurry with 1% of NanoFe with w/c ratio of 0.38 and 0.54 at 25°C and 85°C were modeled. The coefficients of determination (R^2) was greater than 0.97 as summarized in Table 1. The root mean square of error (RMSE) varied between 2.33 Pa and 9.65 Pa based on the temperature, NanoFe content and w/c ratio as summarized in Table 1. Additional of 1% NanoFe to the cement slurry with w/c ratio of 0.38 and 0.54 at 25°C increased the yield stress (τ_{o2}) by 86% and 58% respectively as summarized in Table 1. The model parameter A for the cement slurry with w/c ratio of 0.38 and 0.54 at 25°C and 85°C varied between 0.32 Pa.s^{-1} and 4.7 Pa.s^{-1} as summarized in Table 1. The model parameter B at 25°C and 85°C were 0.004 Pa^{-1} and 0.002 Pa^{-1} respectively, a 50% reduction as summarized in Table 1.

Maximum Shear Stress ($\tau_{max.}$)

Based on Eqn. 5 the hyperbolic model has a limit on the maximum shear stress the slurry will produce at relatively very high rate of shear strains. The τ_{max} for smart cement slurries with 0% and 1% of NanoFe content with w/c ratio of 0.38 and 0.54 at temperature of 25°C were 186 Pa, 74 Pa, 236 Pa and 74 Pa respectively as summarized in Table 1. Increasing the temperatures of smart cement slurries to 85°C increased the maximum shear stress by 108%, 131%, 84% and 413% for smart cement modified using 0% and 1% of NanoFe respectively as summarized in Table 1.

Electrical Resistivity

Based on the current study and past experience of the researchers, the change in resistivity with time can be represented as shown in Fig. 3. Hence several parameters can be used in monitoring the curing (hardening process) of the cement. The parameters are initial resistivity (ρ_o), minimum resistivity (ρ_{min}), time to reach the minimum resistivity (t_{min}), resistivity after 24 hours of curing (ρ_{24}) and percentage of maximum change in resistivity (Resistivity Index) [$RI_{24hr}=(\frac{\rho 24-\rho min)}{\rho min}$]*100]. The test results from various smart cement compositions are summarized in Table 2. The initial electrical resistivity (ρ_o) of smart cement with 0% and 1% of NanoFe with w/c ratio of 0.38 and 0.54 were 1.03 Ω.m, 0.9 Ω.m and 0.87 Ω.m and 0.74 Ω.m respectively, a 18% and 16% for w/c ratio of 0.38 and 0.54 respectively reduction in the electrical resistivity when NanoFe concentration increased by 1% respectively as summarized in Table 2. Also the t_{min} was reduced by 43% and 20% for the w/c ratio of 0.34 and 0.54 respectively when NanoFe concentration increased by 1% as summarized in Table 2. The minimum resistivity (ρ_{min}) of smart cement with 0% and 1% of NanoFe for the w/c ratio of 0.34 and 0.54 were 0.90 Ω.m, 0.77 Ω.m and 0.70 Ω.m and 0.61 Ω.m respectively, a 22% and 21% reduction in the electrical resistivity when NanoFe concentration increased by 1% respectively as summarized in Table 2. The Resistivity index (RI_{24hr}) for smart cement with 0% and 1% of NanoFe with w/c ratio of 0.34 and 0.54 were 279%, 110% and 257%, 105% respectively as summarized in Table 2. These observed trends clearly indicate the sensitivity of resistivity to the changes occurring in the curing of cement (Table 2). Based on experimental results, model proposed by Mebarkia and Vipulanandan (1992) was modified to predict the electrical resistivity of smart cement during hydration up to 7 days of curing a shown in Fig. 5 and Fig. 5. The model is defined as follows:

$$\frac{1}{\rho}=\left(\frac{1}{\rho_{min}}\right)\left[\frac{\left(\frac{t+t_o}{t_{min}+t_o}\right)}{q+(1-p-q)*\left(\frac{t+t_o}{t_{min}+t_o}\right)+p*\left(\frac{t+t_o}{t_{min}+t_o}\right)^{\frac{q+p}{p}}}\right] \qquad (6)$$

where:

ρ: electrical resistivity (Ω-m), ρmin: minimum electrical resistivity (Ω-m), t_{min}: time corresponding minimum electrical resistivity (ρ_{min}), $p = (At + B)$, t_o, A, B and q are model parameters (Table 3) and t: time (min).

Resistivity During the Curing Process

The variation of electrical resistivity with time for smart cement with and without NanoFe is shown in Fig. 4 to Fig. 5. The electrical resistivity initially after mixing dropped to a minimum value (ρ_{min}), and then gradually increased with time. The decrease in electrical resistivity immediately after mixing was due to dissolution of soluble ions from the cement particles after cement is mixed with water, and the dissolving process of the ions causes the resistivity decrease during early period. The time to reach minimum resistivity (t_{min}) can be used as an index of speed of chemical reactions and cement set times. With the formation of resistive solid hydration products which block the conduction path, resistivity increased sharply with curing time. The following increase in electrical resistivity was caused by the formation of large amount of hydration products in the cement matrix. Finally, a relative

stable increase trend is reached by the ions diffusion control of hydration process and resistivity increased steadily up to 24 hours, and reached a value of ρ_{24hr}. Change in electrical resistivity with respect to minimum resistivity, quantifies the formation of solid hydration products which leads to decrease in porosity and hence the strength development. Therefore by tracking the change in resistivity of well cement, a clear understanding of hydration process and strength development can be obtained, which would be valuable in determining the wait on cement times. Variations of electrical resistivity with time for samples with different NanoFe content are summarized in Table 2. Additional of 1% NanoFe had minmal effect on the RI_{24hr}.

Compressive Strength
Effect of NanoFe
1 day of curing

The compressive strength (σ_f) of the cement with w/c ratio of 0.38 and 0.54 modified with 0% and 1% of NanoFe after 1 day of curing were 1583 psi, 763 psi and 1995 psi and 823 psi, a 26% and 9% increase as summarized in Table 4.

28 days of curing

The compressive strength (σ_f) of the cement with w/c ratio of 0.38 and 0.54 modified with 0% and 1% of NanoFe after 28 days of curing were 2810 psi, 1829 psi and 4000 psi and 2159 psi, a 42% and 18% increase as summarized in Table 4.

Piezoresistivity Behavior of Smart Cement

Additional of NanoFe substantially improved piezoresistive behavior of the smart cement.

1 day of curing

The piezoresistive behavior of cement as shown in Fig. 6. After 1 day of curing the piezoresistivity of the smart cement with w/c ratio of 0.38 and 0.54 at failure were 0.72% and 0.48% respectively as summarized in Table 4. Additional of 0.1% CF to the cement increased the change in electrical resistivity of oil well cement at failure $\left(\frac{\Delta\rho}{\rho_o}\right)_f$ with w/c ratio of 0.38 and 0.54 were 583% and 296% respectively as summarized in Table 4. Additional of 1% of NanoFe to the smart cement after 1 day of curing increased the electrical resistivity at failure $\left(\frac{\Delta\rho}{\rho_o}\right)_f$ with different to 700% and 368% respectively as summarized in Table 4. The Piezoresistivity at failure for 1% NanoFe was about 3500 times higher than the compressive strain at failure.

28 days of curing

Additional of 0.1% CF to the cement with w/c ratio of 0.38 and 0.54 increased the change in electrical resistivity of oil well cement at failure $\left(\frac{\Delta\rho}{\rho_o}\right)_f$ as summarized in Table 4. Additional of 1% of NanoFe to the smart cement after 28 days of curing increased the electrical resistivity at failure $\left(\frac{\Delta\rho}{\rho_o}\right)_f$ to 574 % and 328% respectively as summarized in Table 4.

Compressive Strength – Resistivity Relationship

During the entire cement hydration process both the electrical resistivity and compressive strength of the cement increased gradually with the curing time. For cement pastes with various NanoFe content, the change in resistivity was varied during the hardening. The cement paste without NanoFe had the lowest electrical resistivity change (RI_{24hr}), as shown in Table 4.

The relationships between (RI_{24hr}) and the 1 day and 28 day compressive strengths (psi) (Fig. 9) were:

1 day of curing

NanoFe=0%

$$\sigma_{1day} = 3.8 \times RI_{24hr} + 319 \quad (9)$$

NanoFe=1%

$$\sigma_{1day} = 5.2 \times RI_{24hr} + 273 \quad (10)$$

28 day of curing

NanoFe=0%

$$\sigma_{28day} = 4.5 \times RI_{24hr} + 1299 \quad (11)$$

NanoFe=1%

$$\sigma_{1day} = 8 \times RI_{24hr} + 1295 \quad (12)$$

Conclusions

Based on this experimental and analytical study on smart cement with the addition of NanoFe, the following conclusions are advanced:

1. The electrical resistivity responses during curing for various samples followed the same trend. Resistivity reduced to a minimum point, increased sharply and then increased gradually with a lower rate. Therefore, electrical resistivity was a sensitive parameter to monitor the changes during curing of cement
2. Cement with various w/c ratio had different resistivity responses. The change in resistivity was higher for cement with lower water-to-cement ratios.
3. The resistivity index (RI_{24hr}) of the cement with lower w/c ratio was higher than that of the cement with higher w/c ratio. A linear correlation was found between resistivity index and compressive strength at different curing ages.
4. The rheological test showed that class H cement had shear-thinning behavior and a hyperbolic model was proposed to predict shear stress- strain relationship. The model was fitted with the experimental data for cement with several compositions.

5. The smart cement showed piezoresistive behavior. The change in resistivity increased with increasing the compressive stress. Increasing the w/c ratio reduced the piezoresistivity of smart cement at all curing ages.
6. For the smart cement (w/c=0.38) modified with 1% NanoFe, the resistivity change at peak stress was over 2500 times higher than the change in compressive strain.

Acknowledgements

This study was supported by the Center for Innovative Grouting Materials and Technology (CIGMAT) at the University of Houston, Texas. Funding for the project (Project No. 10121-4501-01) is provided through the "Ultra-Deepwater and Unconventional Natural Gas and Other Petroleum Resources Research and Development Program" authorized by the Energy Policy Act of 2005. This program—funded from lease bonuses and royalties paid by industry to produce oil and gas on federal lands—is designed to assess and mitigate risk enhancing the environmental sustainability of oil and gas exploration and production activities. RPSEA is under contract with the U.S. Department of Energy's National Energy Technology Laboratory to administer three areas of research. RPSEA is a 501(c) (3) nonprofit consortium with more than 180 members, including 24 of the nation's premier research universities, five national laboratories, other major research institutions, large and small energy producers and energy consumers. The mission of RPSEA, headquartered in Sugar Land, Texas, is to provide a stewardship role in ensuring the focused research, development and deployment of safe and environmentally responsible technology that can effectively deliver hydrocarbons from domestic resources to the citizens of the United States. Additional information can be found at www.rpsea.org.

References

1. API Recommended Practice 10B (1997), Recommended Practice for Testing Well Cements Exploration and Production Department, 22nd Edition.
2. API Recommended Practice 65 (2002) Cementing Shallow Water Flow Zones in Deepwater Wells.
3. Chung, D. D. L (1995), "Strain Sensors Based on Electrical Resistance Change," Smart Materials Structures, No. 4, pp. 59-61.
4. Chung, D.D.L (2001), "Functional Properties of cement-Matrix Composites," Journal of Material Science, Vol. 36, pp. 1315-1324.
5. Dom, P. B., S. Rabke, et al. (2007). "Development, verification, and improvement of a sediment-toxicity test for regulatory compliance." SPE Drilling & Completion, Vol. 22(2), 90-97.
6. Eoff, L. and Waltman, B. (2009) "Polymer Treatment Controls Fluid Loss While Maintaining Hydrocarbon Flow," Journal of Petroleum Technology, pp. 28-30.
7. Fuller, G., Souza, P., Ferreira, L., and Rouat, D. (2002). "High-Strength Lightweight Blend Improves Deepwater Cementing," Oil & Gas Journal, Vol. 100, No.8, pp. 86-95.
8. Gill, C., Fuller, G. A., and Faul, R. (2005) "Deepwater Cementing Best Practices for the Riserless Section," AADE-05-NTCE-70, pp. 1-14.
9. Labibzadeh, M., Zhhabizadeh, B., and Khajehdezfuly, A. (2010) "Early Age Compressive Strength Assessment of Oil Well Class G Cement Due to Borehole Pressure and Temperature Changes," Journal of American Science, Vol. 6, No.7, pp.38-47.
10. McCarter, W. J. (1996) "Monitoring the influence of water and ionic ingress on cover-zone concrete subjected to repeated absorption", Cement Concrete and Aggregates, 18, pp. 55-63.
11. McCarter, W. J.and Ezirim H. C. (1998) "Monitoring the Early Hydration of Pozzolan-Ca $(OH)_2$ Mixtures Using Electrical Methods" [J]. Advances in Cement Research, 10 (4), pp. 161-168.
12. McCarter, W. J. (2006) "Monitoring the Influence of Water and Ionic Ingress on Cover-Zone Concrete Subjected to Repeated Absorption," Cement, Concrete and Aggregates 18.
13. Mebarkia, S., C., Vipulanandan, (1992) "Compressive behavior of glass-fiber-reinforced polymer concrete, Mater. Civil Engineering, 4, pp. 91–105.
14. Ravi, K. et al. (2007) "Comparative Study of mechanical Properties of Density-reduced Cement Compositions," SPE Drilling & Completion, Vol. 22, No. 2, pp. 119-126.
15. Thaemlitz, J., A. D. Patel, et al. (1999). "New environmentally safe high-temperature water-based drilling-fluid system." SPE Drilling & Completion Vol. 14(3), pp. 185-189.
16. Vipulanandan, C. and Sett, K. (2004) "Development and Characterization of Piezoresistive Smart Structural Materials," Proceedings, Engineering, Construction and Operations in Challenging Environments, Earth & Space 2004, ASCE Aerospace Division, League City, TX, pp. 656-663.
17. Vipulanandan, C. and Liu, J. (2005) "Polyurethane Based Grouts for Deep Off-Shore Pipe-in-Pipe Application", Proceedings, Pipelines 2005, ASCE, Houston, TX, pp. 216-227.
18. Vipulanandan, C.,and Garas, V. (2006), "Piezoresistivity of Carbon Fiber Reinforced Cement Mortar", Proceedings, Engineering, Construction and Operations in Challenging Environments," Earth & Space 2006, Proceedings ASCE Aerospace Division, League City, TX, CD-ROM.
19. Vipulanandan, C. and Garas, V. (2008) "Electrical Resistivity, Pulse Velocity and Compressive Properties of Carbon Fiber Reinforced Cement Mortar," Journal of Materials in Civil Engineering, Vol. 20, No. 2 , pp. 93-101.

20. Vipulanandan, C. and Prashanth, P. (2013) "Impedance Spectroscopy Characterization of a Piezoresistive Structural Polymer Composite Bulk Sensor," Journal of Testing and Evaluation, ASTM, Vol. 41, No. 6, pp. 898-904.
21. Vipulanandan, C., Heidari, M., Qu, Q., Farzam, H. and Pappas, M. (2014a). "Behavior of Piezoresistive Smart Cement Contaminated with Oil Based Drilling Mud." OTC 25200-MS, pp. 1-14.
22. Vipulanandan, C., Krishnamoorti, R., Saravanan, R., Qu, Q. and Narvaez, G. (2014b). "Development and Characterization of Smart Cement for Real Time Monitoring of Ultra-Deepwater Oil Well Cementing Applications." OTC 25099-MS, pp. 1-12.
23. Vipulanandan, C., A. Mohammed, (2014) "Hyperbolic rheological model with shear stress limit for acrylamide polymer modified bentonite drilling muds", Petroleum Science and Engineering, 122, pp. 38–47.

Table 1. Vocadlo and Hyperbolic rheological model parameters for smart cement slurries

			Vocadlo Model (1969)					Hyperbolic Model (2014)					
w/c	NanoFe (%)	T (^oC)	τ_{o1} (Pa)	k ($Pa.s^n$)	n	RMSE (Pa)	R^2	τ_{o2} (Pa)	C ($Pa.s^{-1}$)	D $(Pa)^{-1}$	τ_{max} (Pa)	RMSE (Pa)	R^2
0.38	0	25	20.1	21.3	0.75	5.91	0.98	19.3	1.62	0.006	186	5.7	0.98
		85	42.5	4.6	0.56	11.1	0.98	53.2	0.59	0.003	387	9.9	0.99
	1	25	34.1	18.5	0.67	9.1	0.97	36.2	1.4	0.005	236	8.2	0.99
		85	47.1	56.7	0.61	10.81	0.97	47.0	0.32	0.002	547	9.65	0.98
0.54	0	25	14.9	3.88	0.37	6.2	0.98	15.2	4.25	0.017	74	0.032	0.98
		85	37.5	14.2	0.31	5.6	0.98	36.1	1.01	0.01	136	4.32	0.98
	1	25	21.3	2.9	0.46	2.59	0.98	24.3	4.70	0.02	74	2.33	0.98
		85	41.1	5.99	0.51	5.1	0.99	47.5	1.84	0.003	380	4.33	0.99

Table 2. Summary of bulk resistivity parameters for cement with various w/c ratio and NanoFe content

`w/c	NanoFe (%)	Initial resistivity, ρ_o (Ω.m)	ρ_{min} (Ω.m)	t_{min} (min)	ρ_{24hr} (Ω.m)	$RI_{24\ hr}$ (%)
0.38	0	1.03	0.90	163	3.90	333
	1	0.87	0.70	144	3.0	329
0.54	0	0.90	0.77	145	1.67	117
	1	0.74	0.61	140	1.25	105

Table 3. Model parameters for electrical resistivity of smart cement with different w/c ratio and NanoFe content

w/c	NanoFe (%)	Curing Time (day)	ρ_{min} (Ω.m)	t_{min} (min)	q	t_o (min)	A	B	R^2
0.38	0	1	0.90	168	1.60	130	-0.0001	7.23	0.99
		7			2.20	75	-0.0001	18.8	0.99
	1	1	0.72	135	1.50	178	-0.0001	7.0	0.97
		7			1.97	70	-0.0001	14.0	0.99
0.54	0	1	0.77	96	0.55	86	-0.0001	4.11	0.99
		7			0.57	66	-0.0001	1.44	0.98
	1	1	0.74	90	0.15	85	-0.0001	0.52	0.99
		7			0.70	70	-0.0001	2.0	0.98

Table 4. Variation of piezoresistive behavior for cement with different w/c and NanoFe content

Material	w/c	NanoFe (%)	Curing Time (day)	$(\Delta\rho/\rho o)_f$ (%)	σ_f (psi)
Cement only	0.38	0	1	0.72	1544
			28	0.55	2504
	0.54	0	1	0.48	666
			28	0.33	1635
Smart cement	0.38	0	1	583	1583
			28	401	2810
		1	1	700	1995
			28	574	4000
	0.54	0	1	296	763
			28	271	1829
		1	1	368	823
			28	328	2159

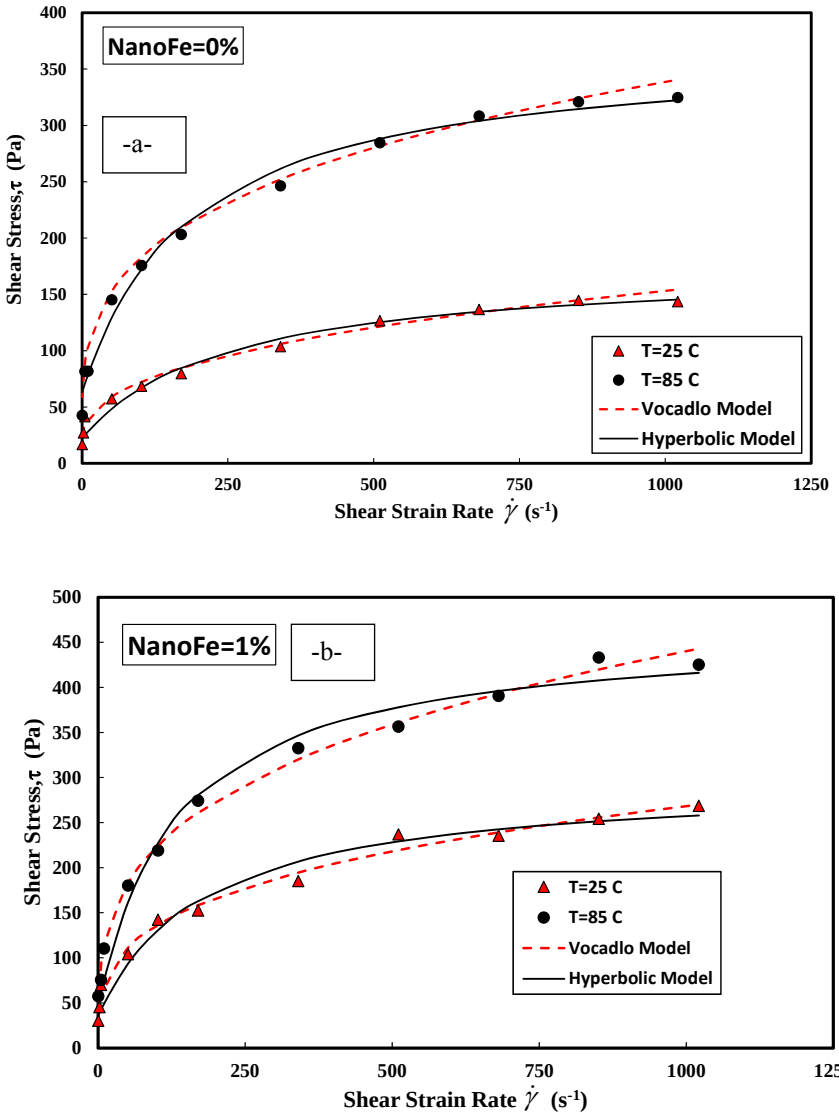

Figure 1: Predicted and measured shear stress - shear strain rate relationship for smart cement slurries with w/c ratio of 0.38 and different temperature (a) NanoFe=0% and (b) NanoFe=1%

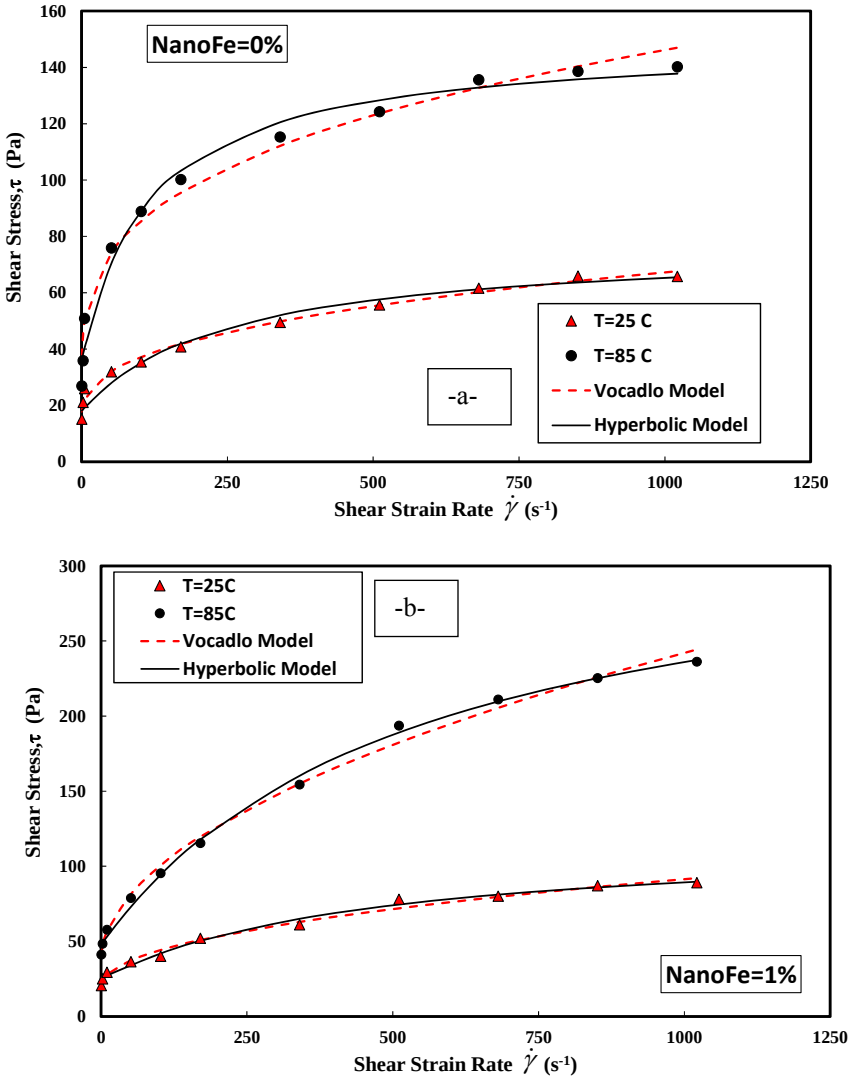

Figure 2: Predicted and measured shear stress - shear strain rate relationship for smart cement slurries with w/c ratio of 0.54 and different temperature (a) NanoFe=0% and (b) NanoFe=1%

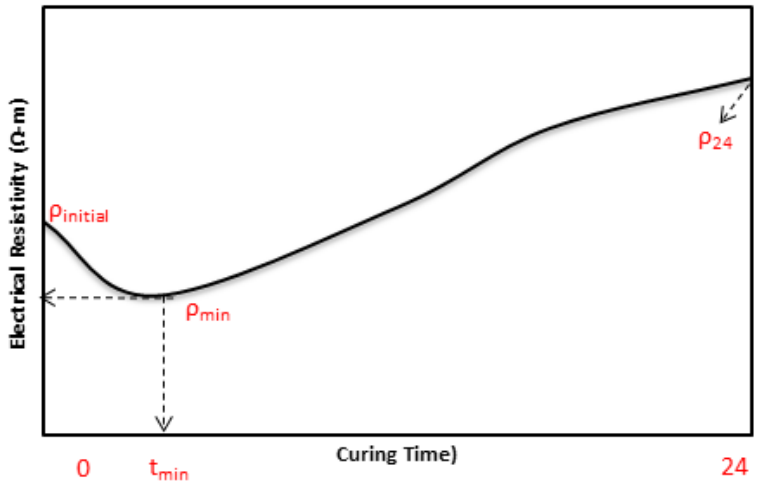

Figure 3. Typical bulk resistivity development with curing time

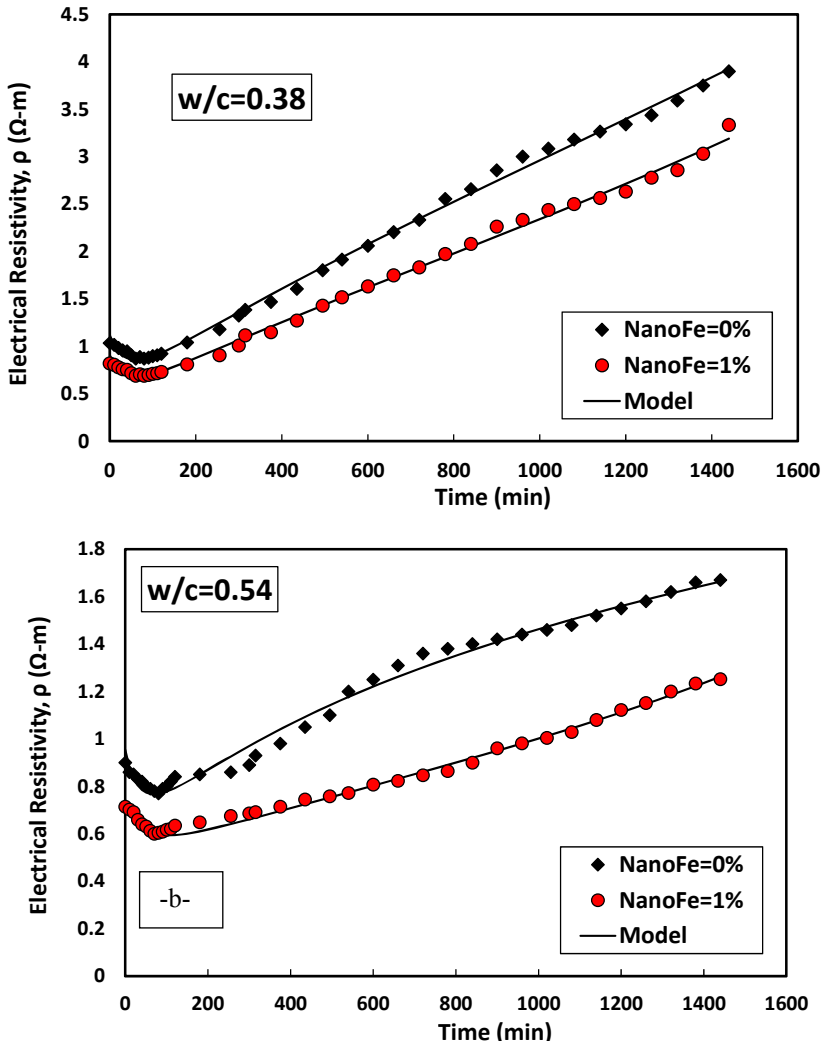

Figure 4: Bulk electrical resistivity development of smart cement for 1 day of curing with various NanoFe content (a) w/c=0.38 (b) w/c=0.54

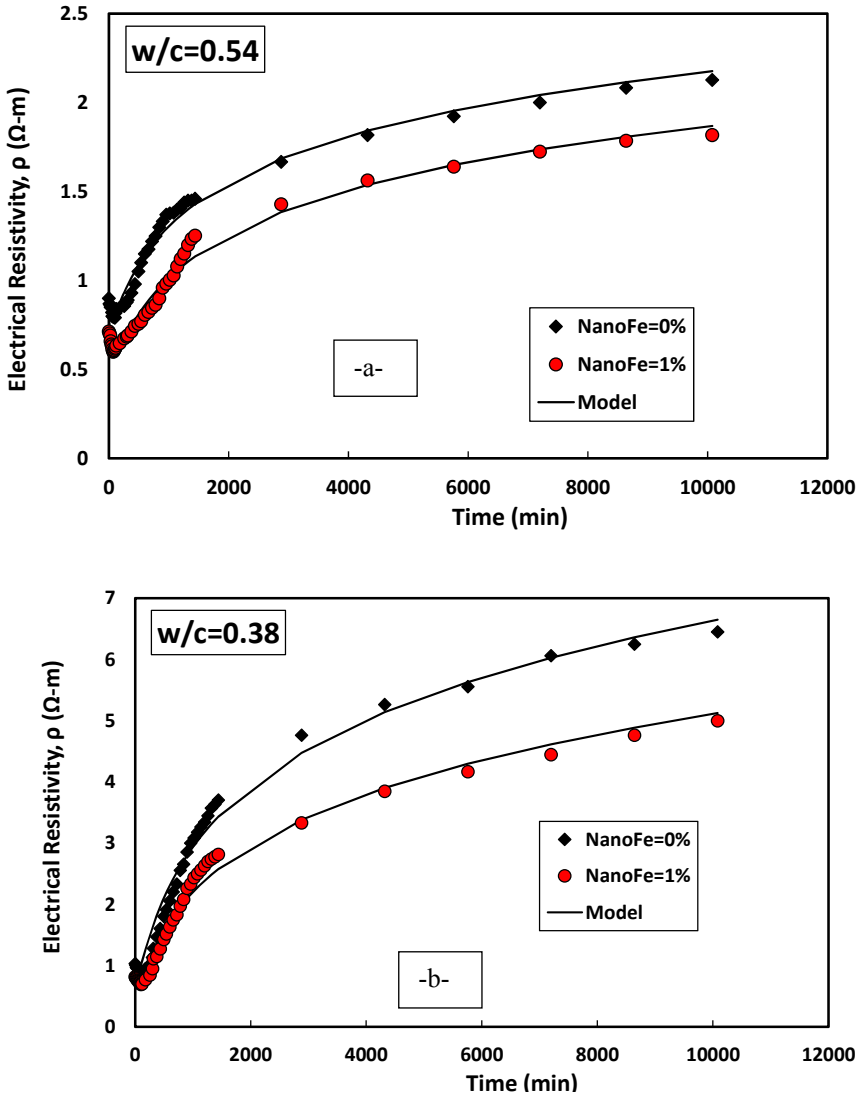

Figure 4: Bulk electrical resistivity development of smart cement for 7 days of curing with various NanoFe content (a) w/c=0.38 (b) w/c=0.54

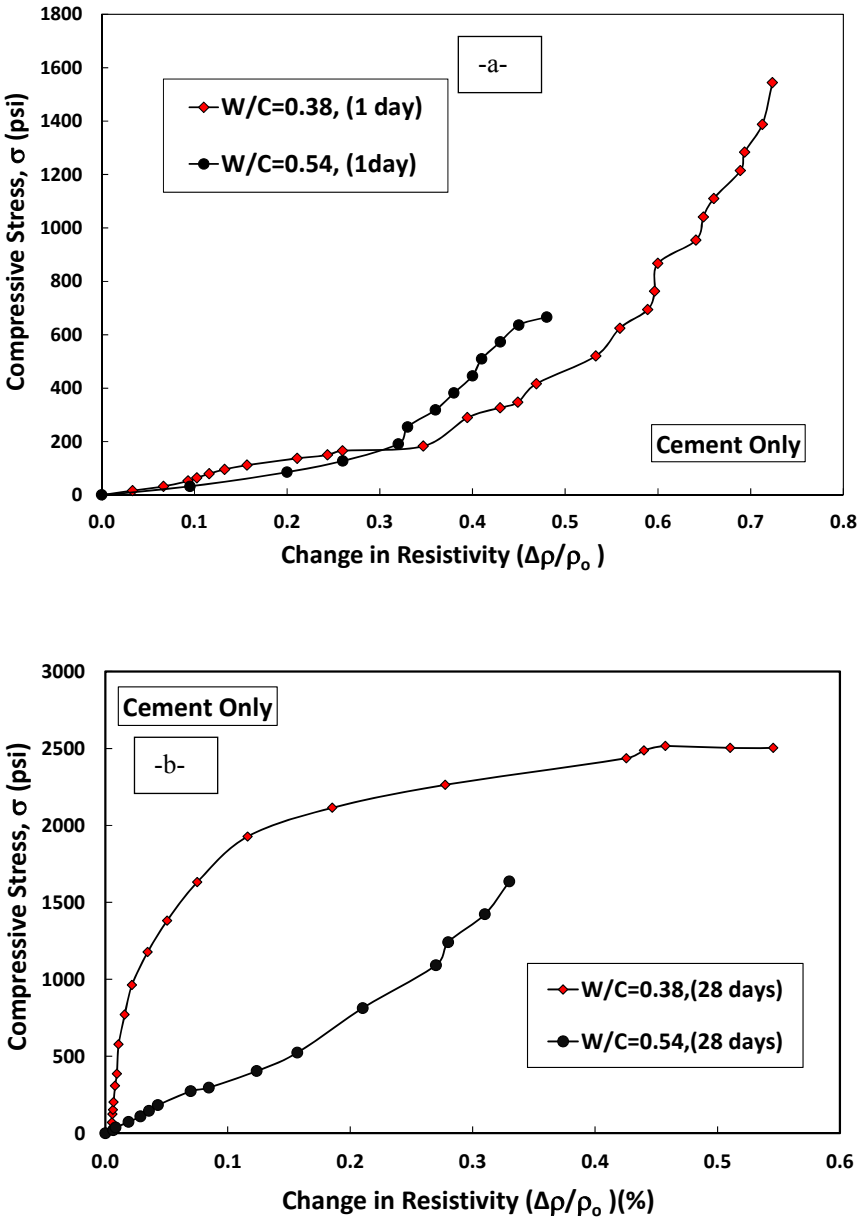

Figure 6: Piezoresistive behaviour of oil well cement with different w/c ratio and curing time (a) 1 day (b) 28 days

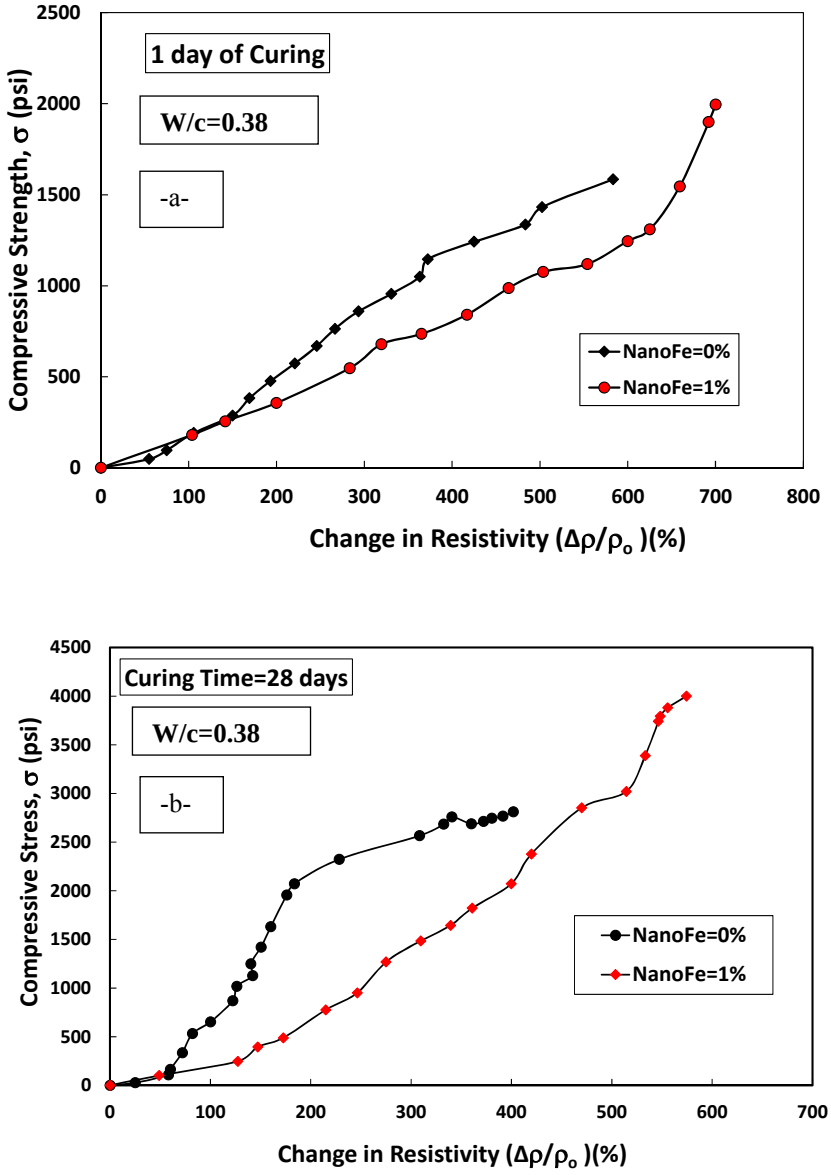

Figure 7: Piezoresistive behaviour of smart cement with different w/c ratio and curing time (a) 1 day (b) 28 days

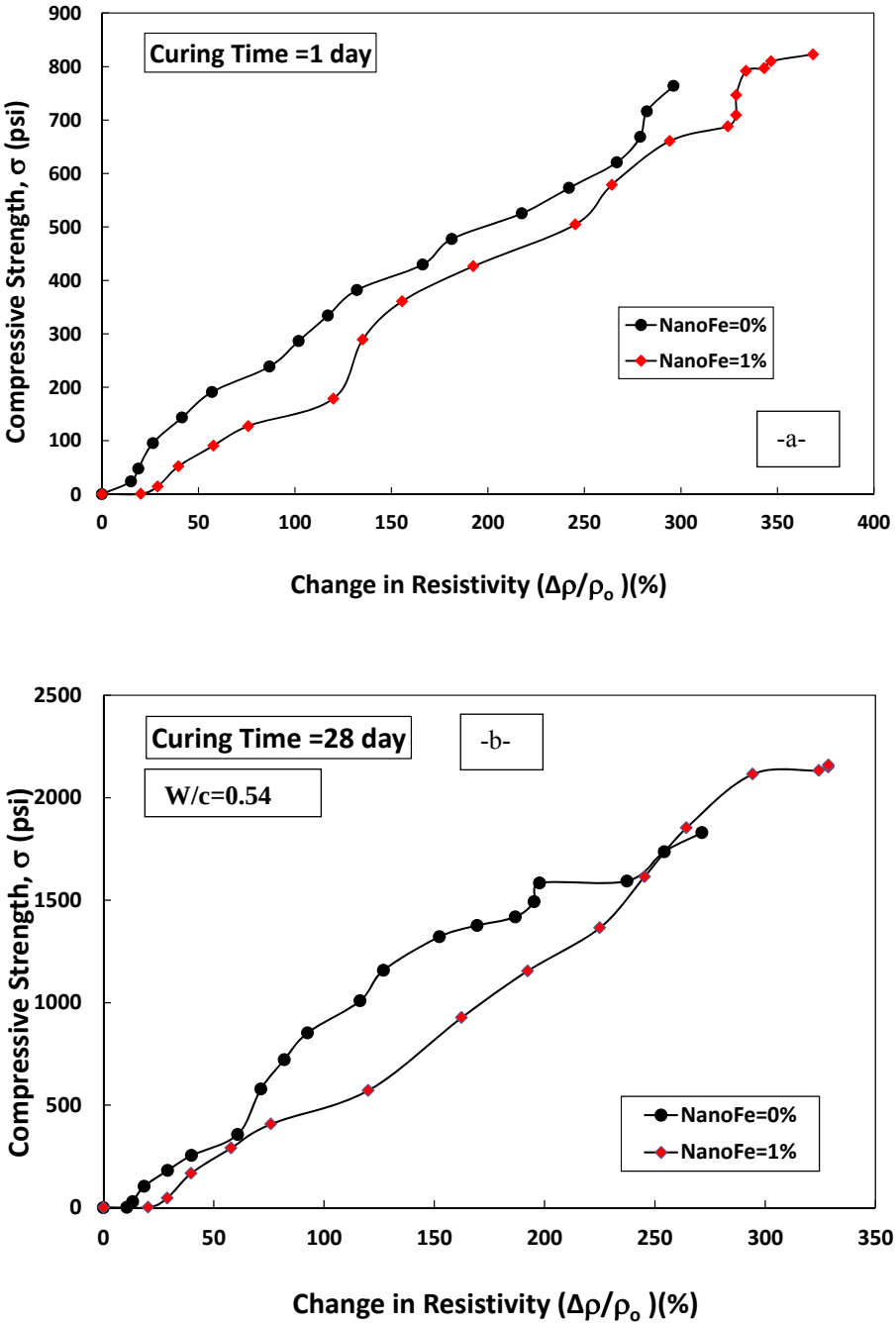

Figure 8: Piezoresistive behaviour of smart cement with different w/c ratio and curing time (a) 1 day (b) 28 days

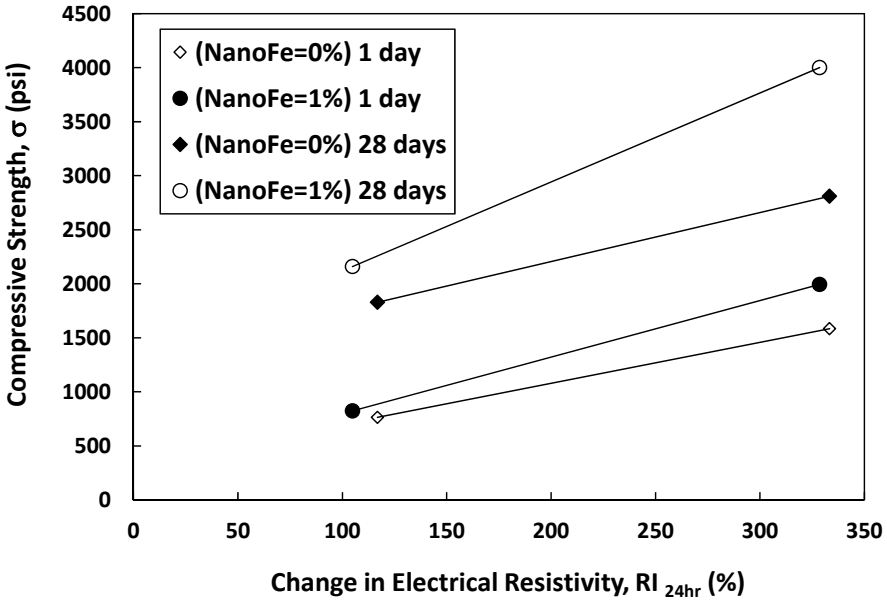

Figure 9. Relationship between resistivity index ($RI_{24\ hr}$) and compressive strength of smart cement modified with NanoFe